Fibers and Polymers 2014, Vol.15, No.10, 2193-2200 DOI 10.1007/s12221-014-2193-5

Analyzing the Quasi-static Puncture Resistance Performance of Shear Thickening Fluid Enhanced P-aramid Composite

H. R. Baharvandi*, P. Khaksari[1], N. Kordani[2], M. Alebouyeh[3], M. Alizadeh[4], and J. Khojasteh[2]

School of Metallurgy and Materials Engineering, University of Tehran, Tehran, Iran
[1]*Ceramic Division, Department of Metallurgy and Materials Engineering, Iran University of Science and Technology, Tehran, Iran*
[2]*Department of Mechanical Engineering, Amir Kabir University of Technology, Tehran, Iran*
[3]*Department of Mechanical Engineering, Science and Research Branch, Islamic Azad University, Tehran, Iran*
[4]*Department of Textile Engineering, South Tehran Branch, Islamic Azad University, Tehran, Iran*
(Received January 29, 2014; Revised April 26, 2014; Accepted May 4, 2014)

Abstract: The quasi-static (QS) puncture resistance of p-aramid Twaron fabric impregnated with shear thickening fluid (STF) based on the molecular weight variation of the base liquid has been investigated. To synthesis the STF, the 12 nm silica particles have been dispersed in polyethylene glycol (PEG) with two different molecular weights, 200 and 400 g/mol by means of mechanical mixing. The weight percentages of silica particles in the continuous phase were selected as 15, 25 and 35 wt%. The results of rheological tests indicate that with the increase of the polymer's molecular weight, the viscosity and instability of the suspension increase, while its critical shear rate diminishes. The STF impregnated Twaron fabrics were subjected to QS puncture resistance tests according to the ASTM standard D6264. The quasi-static puncture resistance increased about 4.5 fold for Twaron fabric impregnated with 35 wt% concentration STF relative to the neat Twaron. Also, with the increase of the PEG's molecular weight in Twaron fabrics impregnated with 15 and 25 wt% concentration STFs, the QS puncture resistance of Twaron fabrics improved considerably, but it didn't change too much in the Twaron fabric impregnated with 35 wt% concentration STF.

Keywords: Shear thickening fluid, Silica nanoparticles, Polyethylene glycol, Quasi static puncture resistance test, P-aramid Twaron fabric

Introduction

Newtonian fluids are those that exhibit a constant viscosity with the increase of shear rate [1]. Shear Thickening Fluids (STFs) are considered as non-Newtonian fluids. The main feature of STFs is that they exhibit an increased viscosity with the increase of shear rate [2,3]. The slope of viscosity increase is an important parameter for shear thickening fluids. If this slope is too steep, it is said that a discontinuous shear thickening has occurred. Discontinuous shear thickening causes the applied force to be absorbed in a very short time [4]. This means that the STF changes from a fluid state to a pseudo-solid state, its viscosity increases rapidly and thus it absorbs the exerted energy.

Through optical analyses of colloidal suspensions, the manner of positioning and distribution of particles in still and stagnant suspensions has been investigated. It has been confirmed that in STFs, in a stagnant state, the particles are distributed in an orderly fashion and this order has a hexagonal form [5].

The order-disorder transition theory and the hydro-cluster formation theory appropriately explain the shear thickening phenomenon.

The order-disorder transition theory attributes the shear thickening phenomenon to the disorder in the arrangement of particles in the fluid caused by the application of shear rate. On the other hand, the hydro-cluster formation theory attributes this phenomenon to the formation of hydro-clusters as a result of hydrodynamic forces overcoming the repulsive steric and Brownian forces [2,6-8].

The shear thickening phenomenon occurs in most of the concentrated colloidal suspensions containing hard solid particles [9]. This behavior has been observed in different fluid mixtures such as clay-water, calcium carbonate-water, polystyrene-silicon oil, iron particles-carbon tetrachloride, titanium oxide-resin, silica-polypropylene glycol and silica-polyethylene glycol [10].

The friction between the yarns and between the fibers and the penetrator greatly affects the puncture resistance of the fabric. During the penetration of a foreign object, the more friction there is between the yarns and between the fibers and the penetrator, the more rupture of fibers is observed than the slipping (sliding) of fibers [11].

One way of improving the resistance and strength of p-aramid fabrics is to increase the friction between the fibers by using shear thickening fluids. By impregnating the fabrics with these fluids, a substantial increase has been observed in the QS puncture resistance of these fabrics [11-14].

This improvement of properties has also been investigated for various types of p-aramid fabrics as well as other fabrics such as nylon. P-aramid fabrics have exhibited a better

*Corresponding author: Baharvandi.h@gmail.com

behavior compared to nylon; and also the properties of fine-woven p-aramid fabrics have improved better than the coarse-woven p-aramid fabrics [15].

Temperature has an influential role in the rheology of polymers and their behavior. The impact of temperature on the shear thickening behavior of polyethylene glycol/silica suspension has been explored and it has been observed that with the rise of temperature, fluid viscosity diminishes and the slope of viscosity increase reduces and as a result, the QS puncture resistance of the aramid/STF composite becomes less [12,16]. The sudden increase of the STF viscosity with a very sharp slope is known as discontinuous thickening.

The behavior of continuous phase has a significant impact on the properties of the STF. polyethylene glycol contains surface OH bonds, and since SiO_2 also has these kinds of bond, hydrogen bonds are formed between polymer chains and particles [17]. With the increase of the molecular weight of fluid, the bridging process between polymer chains and particles intensifies and more hydro-cluster aggregates are formed [18].

Since the continuous phase plays an important role in the behavior of these suspensions and Twaron/STF composites, in this research, the effect of the molecular weight of polyethylene glycol on the rheological characteristics of STFs such as initial and ultimate viscosities and critical shear rate has been studied. Also the effect of the molecular weight of polyethylene glycol on the QS puncture resistance and energy absorption of Twaron/STF composite has been explored.

Experimental

Materials

Polyethylene glycol 200 g/mol (PEG200) and 400 g/mol (PEG400) (Merck, Germany) were used as the continuous phases. Also 12 nm fumed silica particles (Aerosil 200, Evonik, Germany) were used for dispersion in the polymer medium.

The other component of this composite is Twaron type D2200 fabric with a areal density of 235 g/m^2. Twaron is a high-strength low-weight fabric with a plain weave made of p-aramid fibers.

Synthesis the STF Samples

The samples were made at three different weight percentages of nanoparticles in the suspension (three different concentrations). For both molecular weights of PEG200 and PEG400, 15, 25 and 35 wt% samples were prepared by dispersing the particles into the polymer using a 10 hp mechanical mixer rotating at 5700 rpm. The mixing continued until achieving a homogeneous and stable suspension. After preparing the suspension, it was left undisturbed at room temperature for 24 hours in order to expel the air bubbles.

Preparation the P-aramid/STF Composite

For a better infusion of the STF suspension into the fibers, the STF was diluted with absolute ethanol in proportions of 1:3 (STF:ethanol). The 152×152 mm fabrics were soaked inside the STF-ethanol solution for 2 minutes and then the samples were put under pressure by a 5 kg cylindrical roller. Afterwards the samples were placed in a drying oven for 25 minutes at a temperature of 60 °C in order to expel the added ethanol from the fabric and obtain the Twaron/STF composite. For both molecular weights of PEG, the average weight of absorbed STF in the fabric at 15, 25 and 35 wt% samples were about 21, 25 and 29 %, respectively.

Characterization

The STF samples were tested for its rheological properties by using the Anton Paar Phisica Rheometer-MCR 300. The shear rate sweep, strain sweep and frequency sweep tests were performed on the samples. The diagrams of viscosity versus shear rate, dynamic modulus versus strain and dynamic modulus versus frequency were prepared. These diagrams were obtained in the CP-50 mode.

The QS puncture test was conducted based on the ASTM standard D6264 by the INSTRON 1484 testing machine, at a speed of 6 mm/s. In this test, to apply the concentrated load on the surface of the 152×152 mm fabric, a steel Rounded edge penetrator with a diameter of 12.7 mm and length of 25 mm has been used. The QS puncture resistance of Twaron/STF composite fabrics was investigated in this experiment.

Fabric is fixed between 2 steel frames with a thickness of 40 mm and length and width of 200 mm. In the center of the steel frames, there is a blank circular space with a diameter of 127 mm for the application of load. The two frames are toughly joined together by 4 screws. In order to have no space left between the fabric and frames, an O-ring is used to prevent the fabric slippage during puncture test. Hence boundary conditions of fabric consider to be fully fixed in all directions.

Figure 1 shows the apparatus for the quasi-static puncture test and the fabric sample being deformed by the rounded edge penetrator.

The images produced by the Philips XL30 scanning electron microscope have been used to observe the impregnation of the fabrics with the STF.

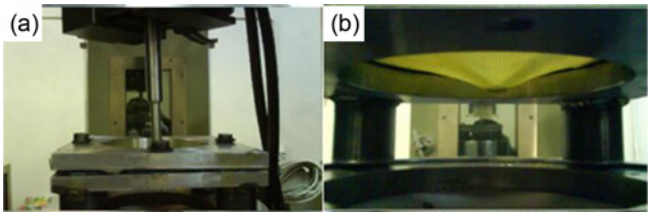

Figure 1. Quasi-static puncture test; (a) the INSTRON test machine and (b) Twaron sample during the applied load.

Results and Discussion

In Figures 2 through 4, the shear rate sweep diagrams for STF suspensions with weight percentages of 15, 25 and 35 wt% containing 12 nm silica particles dispersed in PEG200 and PEG400 have been presented and compared.

Figure 2 compares the shear rate sweep curves of STF samples with 15 wt% concentration for both the PEGs with molecular weights of 200 and 400 g/mol. The viscosity of the PEG400 supension is 10 Pa.s at a shear rate of 1.0 s^{-1}, which diminishes to about 1.0 Pa.s with the increase of the shear rate. At the shear rate of 35 s^{-1}, viscosity jumps to about 100 Pa.s; in other words, discontinuous shear thickening occurs at the shear rate of 35 s^{-1}.

As is observed in Figure 2, in the shear rate range of 1-100 s^{-1}, the PEG200 suspension doesn't enter the shear thickening region and it displays a reduced viscosity in this range, with the increase of shear rate. For this sample, the shear thickening occurs after the shear rate of 100 s^{-1}.

The shear rate sweep curves of STF samples with 25 wt% concentration for both the PEGs with molecular weights of 200 and 400 g/mol are illustrated in Figure 3 for the shear rate range of 0.1-100 s^{-1}. The viscosity of the PEG400 suspension is equal to 180 Pa.s at the shear rate of 0.1 s^{-1}, which reduces almost linearly to a viscosity of 4.5 Pa.s. The shear thickening phase begins at a shear rate of about 20 s^{-1} and the ultimate viscosity goes up to a value of 350 Pa.s.

By examining Figure 3, it is observed that the PEG200 suspension has a higher critical shear rate and a sharper slope of viscosity increase. Also, in the STF samples with 25 wt% concentration, like in the 15 wt% concentration STF samples, the initial and ultimate viscosities are greater in the PEG400 suspension.

As Figure 4 shows, the shear rate sweep tests have been carried out for the STF samples with 35 wt% concentration for both the PEGs with molecular weights of 200 and 400 g/mol at shear rates between 0.01 and 10 s^{-1}. The initial viscosity of the PEG400 suspension is about 1100 Pa.s, which reduces almost linearly to a viscosity of 55 Pa.s. The shear thickening phase begins at a shear rate of about 10 s^{-1} and the ultimate viscosity increases to about 700 Pa.s. Similar to STF samples with 15 and 25 wt% concentrations, as the molecular weight of the continuous phase goes up in this STF sample, the initial, critical and the ultimate viscosities of the STF increase, the slope of viscosity increase in the shear thickening region becomes less and the critical shear rate of STF diminishes.

As was previously observed, the STF samples made of polyethylene glycol with greater molecular weight have higher initial, ultimate and critical viscosities. The reason is the existence of longer molecular chains that inhibit the relative movement of adjacent layers of fluid relative to each other.

In Figures 2 through 4, it was demonstrated that the slope of viscosity increase in the shear thickening region is steeper in the PEG200 suspension; because the viscosity of PEG200

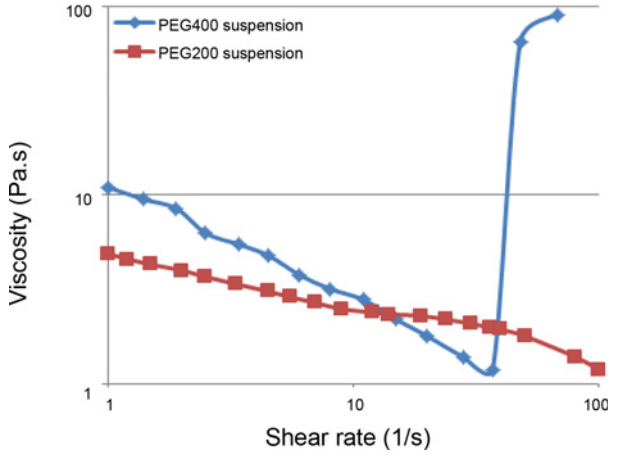

Figure 2. Shear rate sweep curves for both the PEG200 and PEG400 suspensions with 15 wt% concentration.

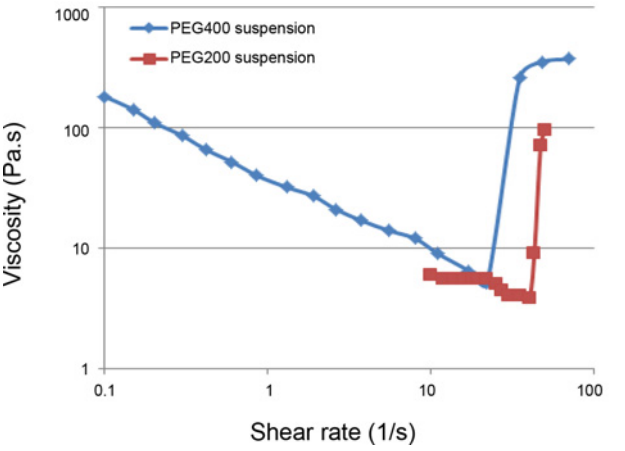

Figure 3. Shear rate sweep curves for both the PEG200 and PEG400 suspensions with 25 wt% concentration.

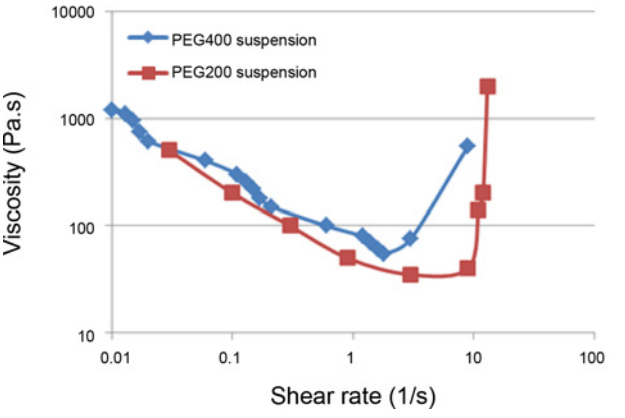

Figure 4. Shear rate sweep curves for both the PEG200 and PEG400 suspensions with 35 wt% concentration.

is lesser than that of PEG400. In other words, the molecular chains in PEG200 are shorter and thus movement prohibition of aggregates in the PEG200 is lesser. Therefore, the aggregates can move faster in PEG200 suspension, and the clusters are formed more quickly.

It was also observed that the increase in the molecular weight of the continuous phase (increase in the length of the molecular chains of the PEG) leads to the reduction of the critical shear rate value. Due to the presence of OH bonds on the surface of silica particles and also the presence of this type of bond in the polyethylene glycol, the formation of hydrogen bonds is plausible. The same hydrogen bonds between polymer chains and particle surfaces cause the adsorption of particles. Therefore, with longer polymer chains, the bridging process becomes easier, and larger aggregates are formed and naturally, less energy is needed to bring these aggregates closer and join them together to form clusters; Thus, a lower shear rate is needed for the onset of shear thickening [19-23].

In other words, the effective silica volume fraction in PEG400 is higher than in PEG200. Silica primary agglomerates moving through PEG400 molecular chains suffer much more difficulties. So in PEG400 suspension, as the aggregates have greater sizes, a lower hydrodynamic energy to develop cluster sizes big enough to increase the viscosity by dominating hydrodynamic lubrication forces is needed. i.e., due to the presence of agglomerates with bigger volume, the critical shear rate is achieved at a lower value [8].

As it was shown, the sudden increase of viscosity at higher strains is due to the shear thickening phenomenon, which is in accordance with the hydro-clusters formation theory.

Figure 5 shows the curves of dynamic modulus versus strain for the STF samples with 15 wt% concentration in two types of PEGs with molecular weights of 200 and 400 g/mol. The measurements have been taken at the constant frequency of 10 s^{-1} and variable strains.

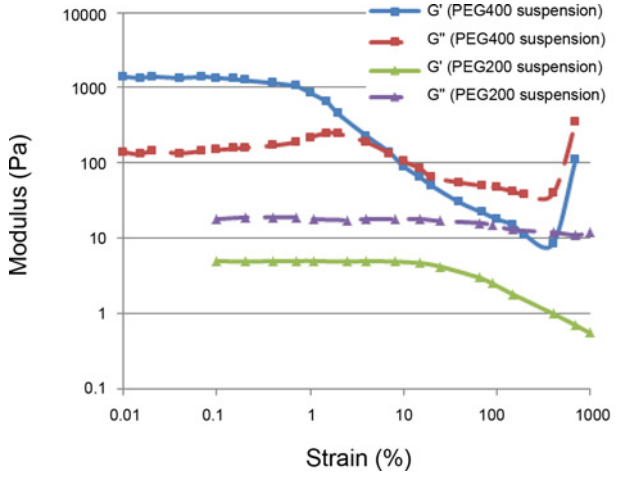

Figure 5. Strain sweep curves for both the PEG200 and PEG400 suspensions with 15 wt% concentration.

In the PEG200 suspension, at all strains, viscous modulus G'' is higher than elastic modulus G', which indicates the dominance of the viscous state over the elastic state in the suspension, and shows the stability of the suspension. The viscous modulus indicates the liquid-like behavior of the suspension, while the elastic modulus points to its solid-like behavior. The predominance of the elastic state over the viscous state means the instability of the suspension. In this sample, with the increase of strain up to 1000 %, no slope increase (shear thickening) is observed in any of the viscous modulus and elastic modulus curves. For this sample, the shear thickening occurs after the strain of 1000 %.

For the PEG400 suspension, at strains less than 8 %, the elastic modulus curve (G') is situated higher than the viscous modulus curve (G''). Therefore, this sample has the elastic behavior at low strains. It should be mentioned that, the more vertical distance there is between two curves, a more solid-like behavior will be expected from the suspension. With the increase of strain and passing the 8 % strain point, the viscous modulus curve stands higher than the elastic modulus curve; and this means the stabilization of the sample. From the 8 % strain point up to a strain of 500 %, the slope of the G' curve diminishes more than the slope of the G'' curve. In this range, the shear thinning phenomenon has occurred. From the strain of 500 % onward, the curves of G' and G'' increase with a very steep slope, which means the occurrence of shear thickening.

In view of Figure 6, in the PEG200 suspension with 25 wt% concentration, in all ranges of strain up to 1000 %, the viscous modulus is higher than the elastic modulus, and the suspension is stable. However, shear thickening is observed in this range.

In the PEG400 suspension with 25 wt% concentration, at strains lower than 24 %, the curve of elastic modulus G' stands higher than that of viscous modulus G'', which means that the sample has a solid-like behavior at low strains. With

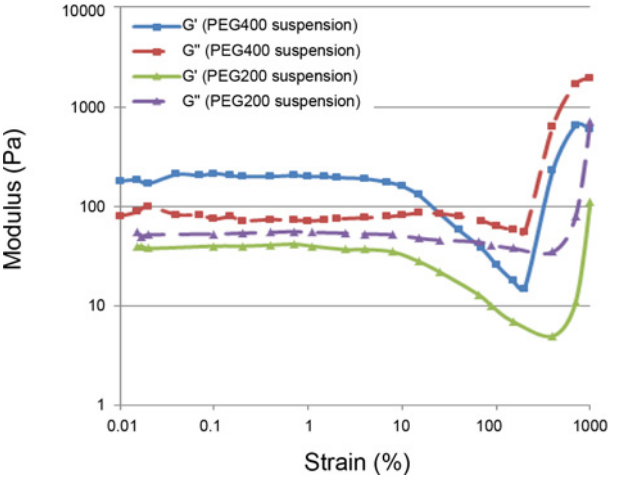

Figure 6. Strain sweep curves for both the PEG200 and PEG400 suspensions with 25 wt% concentration.

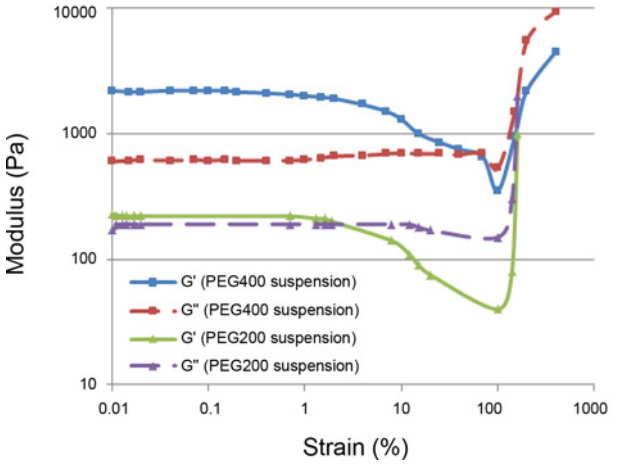

Figure 7. Strain sweep curves for both the PEG200 and PEG400 suspensions with 35 wt% concentration.

the increase of strain, the viscous modulus curve goes above the elastic modulus curve, which means the stabilization of the sample at high strains.

Figure 7 illustrates the STF samples with 35 wt% concentration in two types of PEGs with molecular weights of 200 and 400 g/mol. in the 35 wt% PEG200 suspension, it is observed that, contrary to 15 and 25 wt% samples, the elastic modulus is a little higher than the viscous modulus, at low strains, which means that the stability of the suspension has diminished relative to STF suspensions with less concentrations.

As usual the PEG400 suspension with 35 wt% concentration displays the elastic behavior at low strains. With the increase of strain and passing the 70 % strain point, the curve of viscous modulus stands higher than the elastic modulus curve, which means the stabilization of the sample.

Generally, in all the strain sweep curves, it is observed that the modulus values of PEG400 suspensions are higher than those of PEG200 suspensions. The reason is that, because of the longer molecular chains and the higher effective silica volume fraction in PEG400, not only more aggregates are formed in the suspension, but also these chains more extensively prevent the relative movement of fluid layers.

The increase in the molecular weight of polyethylene glycol means longer molecular chains, higher possibility of bridging between polymer and particles, larger aggregates formation in the suspension and the transition from the viscous state to elastic state. A better load transfering capability is the characteristic of elastic state in the STFs. In the PEG400 suspension, due to larger aggregates that exist in the suspension, the suspension can transfer more load, and the elastic state prevails. That's why the suspension becomes less stable by increasing the molecular weight of polyethylene glycol [19-24].

Similar to the analysis presented for the shear rate sweep diagrams, in the PEG400 suspension, in comparison with

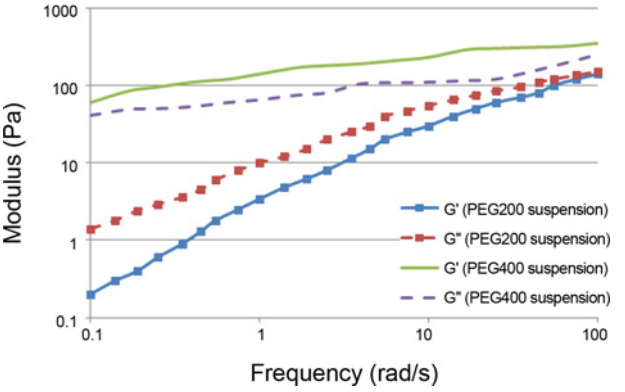

Figure 8. Frequency sweep curves for both the PEG200 and PEG400 suspensions with 25 wt% concentration.

PEG200 suspension, shear thickening begins at lower strains. In other words, critical strain value diminishes in the suspension containing higher molecular weight PEG.

In all three Figures 5, 6 and 7, the greater reduction in the slope of G' curve relative to G'' curve in the shear thinning region means that, with the increase of strain value, not only no new hydro-cluster structure is formed, but also the sample becomes more viscous, and the few initial networks in it collapse.

At the point where the curves of two modulus intersect, the elastic and pseudo-solid structure of the suspension breaks down and after that point, G' becomes less than G''.

Here also, the sudden increase of elastic and viscous modulus at higher strains is due to shear thickening, which is in accordance with the hydro-clusters formation theory.

At high strains, G' and G'' curves get very close to each other. This means that the behavior of suspension in this range of strains, is close to the viscoelastic state.

Figure 8 shows the frequency sweep curves for STF samples with 25 wt% concentration in two types of PEGs with molecular weights of 200 and 400 g/mol, at a constant strain of 1 %. With the increase of frequency for the PEG200 suspension, the curve of G'' is initially higher than the curve of G', which indicates the viscous state and the stability of the suspension. As the frequency increases, so do the values of both modulus; however, the slope of G' increase is sharper than the slope of G'' increase. At the frequency of 100 (rad/s), the two diagrams approach each other and cross at one point. However, beyond this point, G' rises above G'' and the suspension's elastic state prevails. This is the point where linked hydro-cluster networks are formed and shear thickening takes place.

As is observed in Figure 8, in the PEG400 suspension, at all frequencies, the G' curve is above that of G'', which indicates the dominance of the elastic state in the suspension. Therefore, this diagram also demonstrates that the suspension made of higher molecular weight PEG is less stable and enters the shear thickening region sooner.

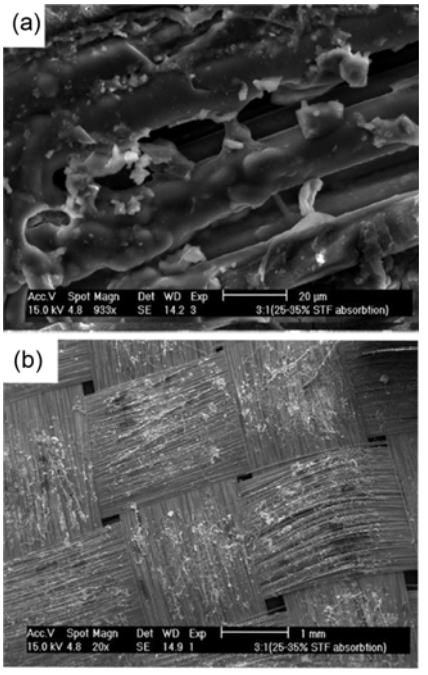

Figure 9. Scanning electron microscope images of Twaron fabric impregnated with PEG200 suspension with 25 wt% concentration; (a) at ×20 magnification and (b) at ×933 magnification.

Figure 9 shows the scanning electron microscope images of Twaron fabric impregnated with PEG200 suspension at 25 wt% concentration. As is observed, the suspension has been distributed uniformly throughout the fabric and infiltrated into the fibers.

In Figure 10, the diagrams obtained from the QS puncture tests for neat Twaron and also Twaron fabrics impregnated with STF with 15 wt% concentration have been presented and the effect of molecular weight of PEG on the QS puncture resistance has been investigated. All puncture test results have been obtained with five-repetition.

From Figure 10, it is observed that the PEG400 suspension impregnated Twaron has the highest tolerable load (2423 N) and the most displacement before yielding (45 mm) in the three samples. In the PEG200 suspension impregnated Twaron, the maximum tolerable load is 2001 N and the maximum displacement before yielding is 48 mm. By yielding, we mean the complete passing of the penetrator through the composite. As the Figure 10 shows, in 15 wt% concentration, the increase in the PEG's molecular weight has led to nearly 20 % increase in the load needed for yielding in the composite, and the displacement before yielding has also increased. Moreover, for both the PEG400 and PEG200 suspensions impregnated Twaron fabrics, a considerable increase (132 % and 181 % for PEG200 and PEG400 suspensions impregnated Twaron fabrics, respectively) can be seen in the amounts of maximum tolerable loads relative to the neat Twaron.

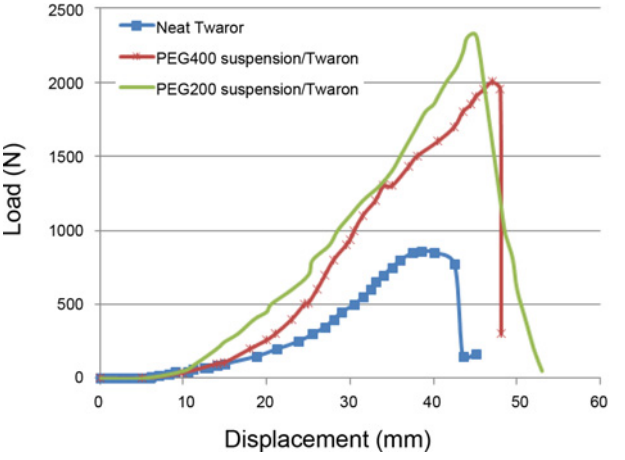

Figure 10. Load-displacement diagrams for Twaron fabrics impregnated with 15 wt% concentration STFs for both the PEG200 and PEG400 suspensions.

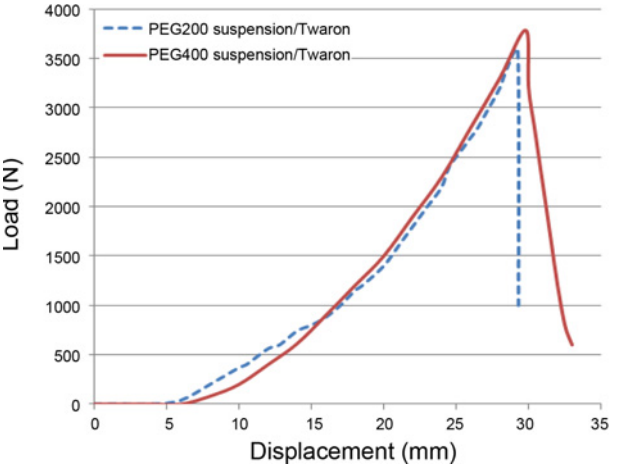

Figure 11. Load-displacement diagrams for Twaron fabrics impregnated with 25 wt% concentration STFs for both the PEG200 and PEG400 suspensions.

In view of Figure 11, the largest displacement before yielding (29.8 mm) and the highest tolerable load (3787 N) have been obtained for the PEG400 suspension impregnated Twaron in the three samples. In the PEG200 impregnated Twaron suspension, the maximum displacement before yielding and the maximum tolerable load have been obtained as 29.2 mm and 3581 N, respectively. As is observed, in both the PEG200 and PEG400 suspensions impregnated Twaron fabrics, the displacement before yielding is almost the same; however, similar to the 15 wt% samples, in the 25 wt% samples also, the PEG400 suspension impregnated Twaron displays a higher QS puncture resistance. In this sample, also, for both the PEG400 and PEG200 suspensions impregnated Twaron fabrics, a substantial increase (315 % and 339 % for PEG200 and PEG400 suspensions impregnated Twaron fabrics, respectively) can be seen in the amounts of

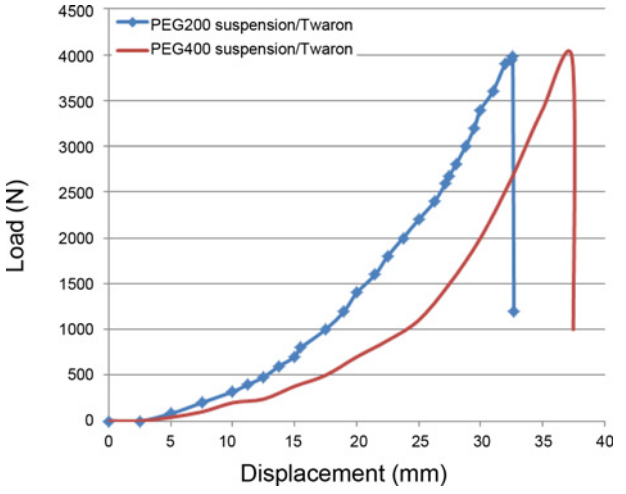

Figure 12. Load-displacement diagrams for Twaron fabrics impregnated with 35 wt% concentration STFs for both the PEG200 and PEG400 suspensions.

Table 1. Maximum absorbed energy, maximum tolerated load before yielding and maximum displacement before yielding for the neat and impregnated Twaron fabrics in the 15, 25 and 35 wt% silica concentrations for both the PEG200 and PEG400 suspensions

Samples	Maximum displace-ment (mm)	Maximum load (N)	Yield energy (J)
Neat Twaron	43	863	14
15 wt% - PEG200 suspension/Twaron	48	2001	34
15 wt% - PEG400 suspension/Twaron	45	2423	37
25 wt% - PEG200 suspension/Twaron	29.2	3581	30.3
25 wt% - PEG400 suspension/Twaron	29.8	3787	32
35 wt% - PEG200 suspension/Twaron	32.6	3983	40.25
35 wt% - PEG400 suspension/Twaron	37.4	3963	37.5

maximum tolerable loads relative to the neat Twaron.

It is observed from Figure 12, that the largest displacements before yielding is 37.4 mm and 32.6 mm and the maximum tolerable loads is 3963 N and 3983 N for the PEG400 and PEG200 suspensions impregnated Twaron fabrics, respectively. It can be seen that, in the sample with higher molecular weight suspension, the amount of displacement before yielding is greater; but the QS puncture resistances of the two samples are not much different. In this concentration, also, for both the PEG400 and PEG200 suspensions impregnated Twaron fabrics, a sizeable increase (about 360 %) can be seen in the amounts of maximum tolerable loads relative to the neat Twaron.

The results of load-displacement diagrams for the neat and impregnated Twaron fabrics in the three silica concentrations for both the PEG200 and PEG400 suspensions have been presented in Table 1.

According to Table 1, It can be understood that when a penetrator enters a neat fabric, the strain produced at the location of impact is transferred along the fibers to the edges of the fabric. Due to a lack of sufficient friction between the fibers of the neat fabric, these fibers slide (slip). So the penetrator passes through the fibers easily by pushing aside them. In the STF impregnated fabric, the silica nanoparticles existing in the fibers prevent the fibers from sliding easily [25]. When a load is applied to the STF impregnated fabric, especially in the case of high concentration STFs, the silica nanoparticles can play a positive role in increasing the friction by filling the openings between the fibers and between the gaps where the fibers cross and prevent the sliding of the fibers easily. In the STF impregnated fabric, the penetrator is able to passes through the fabric by a combination of tearing the fibers and pushing them aside.

Moreover, because of the increase of the STF viscosity during the application of a load, the STF impregnated fabrics absorb some part of the energy. This increase of viscosity also increases the friction and reduces the sliding of the filaments in the fibers and at the locations where the fibers cross, and ultimately improves the QS puncture resistance of the sample.

Shear thickening occurs even in quasi-static puncture tests. The transitional behavior of a STF is fundamentally triggered by critical stress levels [26]. Normalizing the typical puncture force by penetrator tip surface area provides tentative value of shear stress within the fabric of 10^6-10^7 Pa, high enough to induce transition (many orders of magnitude higher than STF transitional stresses of ~10-10000 Pa). Therefore, the stresses encountered by the STFs intercalated in the small gaps between the fibers are likely to be sufficient to trigger shear thickening [26].

According to the hydro-cluster formation theory, it has considered the formation of hydro-clusters due to the prevailing of the hydrodynamic forces over the repulsive steric and Brownian forces as the cause of shear thickening phenomenon. In other words, the shear thickening phenomenon can be described by the transition of the particles' micro-structure from an equilibrium state (which has been established through the repulsive Brownian force) to a flocculated (agglomerated) state [8,24].

During static load, based on the non-Newtonian and nonlinear reaction of the STF intercalated between the fibers (hydro-cluster formation theory), the nanoparticles which there are in the STF, accumulate around the load application point, and the viscosity of the STF increases. The nonlinear increase of STF viscosity causes a considerable increase of friction between fabric and penetrator, between fibers themselves and between the yarns at their crossing points. This way, the fibers better keep their order, and the penetrator encounters a higher resistance by the coated fabric when trying to push aside (windowing) and pull out the yarns.

By looking at the QS puncture test results (Table 1), it is observed that in the Twaron fabrics impregnated with 15 and

25 wt% concentration STFs for both the PEG200 and PEG400 suspensions, the increase in the molecular weight of polyethylene glycol, increases significantly the QS puncture resistance of the fabrics; Because by increasing the molecular weight of the PEG, the initial, critical and the ultimate viscosities of the STF, friction between fibers themselves and also between fibers and the penetrator increases. But in the fabrics impregnated with 35 wt% concentration STFs for both the PEG200 and PEG400 suspensions, because of the high viscosity of high concentration STFs, the variation of the molecular weight of the PEG has little effect on the QS puncture resistance increase of the composite. Because viscosity changes resulting from the increase of the molecular weight of the PEG is insignificantly in contrast to the high viscosity of each suspension [15,27-29].

The QS puncture resistance of the Twaron fabric impregnated with 35 wt% concentration STF shows an almost 4.5 fold improvement relative to that of the neat Twaron. Also, the energy absorbed by this composite has increased almost 2.7 fold compared to the neat Twaron. As was mentioned above, the reason for more energy absorption is the increase of STF viscosity and the increase of friction between fibers themselves and also between fibers and the penetrator [15,27-29].

Conclusion

The following conclusions can be made regarding the findings of this paper:

1. Suspensions containing a polyethylene glycol with higher molecular weight are less stable.
2. The increase in the molecular weight of polyethylene glycol increases the viscosity of the suspension and reduces the critical shear rate.
3. The QS puncture resistance of the Twaron fabrics impregnated with 35 wt% concentration STFs shows an almost 4.5 fold improvement relative to that of the neat Twaron.
4. The increase in the molecular weight of polyethylene glycol in the Twaron fabrics impregnated with 15 and 25 wt% concentration STFs improves considerably the QS puncture resistance of the fabrics; But in the Twaron fabrics impregnated with 35 wt% concentration STFs, by increasing the molecular weight of polyethylene glycol, the QS puncture resistance doesn't change too much.

References

1. R. C. Neagu, P. Bourban, and J. E. Manson, *Comp. Sci. Tech*., **69**, 515 (2009).
2. M. Astruc and P. A. Navard, *J. Rheol.*, **44**, 4693 (2000).
3. A. Krajnc, Ph.D. Dissertation, University of Ljubljana, Ljubljana, Slovenia, 2011.
4. G. Bettin, M.Sc. Dissertation, University of California, Berkeley, USA, 2005.
5. M. Tomita and T. G. M. van de Ven, *J. Colloid Interf. Sci.*, **99**, 374 (1984).
6. E. D. Wetzel, Y. S. Lee, R. G. Egres, K. M. Kirkwood, J. E. Kirkwood, and N. J. Wagner, "Proceedings of 14th International Conference on Composite Materials", pp.1513-1531, 2003.
7. I. M. Krieger and T. J. A. Dougherty, *Trans. Soc. Rheol*., **3**, 137 (1959).
8. F. J. G. Rosales, F. J. R. Hernandez, and J. F. V. Navarro, *Rheol. Acta*, **48**, 699 (2009).
9. H. A. Barnes, "An Introduction to Rheology", 1st ed., pp.93-110, Elsevier Science Publications, Amsterdam, Netherland, 1989.
10. A. H. Tarig, K. R. Vijay, and S. Jeelani, *Mater. Sci. Eng. A*., **527**, 2892 (2010).
11. V. B. C. Tan, T. E. Tay, and W. K. Teo, *Int. J. Solids. Struct*., **42**, 1561 (2005).
12. A. Srivastava, A. Majumdar, and B. S. Butola, *Mater. Sci. Eng. A*, **529**, 224 (2011).
13. D. P. Kalman, J. B. Schein, J. M. Houghton, C. H. N. Laufer, E. D. Wetzel, and N. J. Wagner, "Proceedings of SAMPE 2007", pp.893-901, 2007.
14. E. V. Lomakin, P. A. Mossakovsky, and A. M. Bragov, *Arch. Appl. Mech*., **81**, 2007 (2011).
15. M. J. Decker, C. J. Halbach, C. H. Nam, N. J. Wagner, and E. D. Wetzel, *Com. Sci. Tech*., **67**, 565 (2007).
16. M. C. Newstein, H. Wang, N. P. Balsara, A. A. Lefebvre, Y. Shnidman, H. Watanabe, K. Osaki, T. Shikata, H. Niwa, and Y. Morishima, *Chem. Phys*., **111**, 4827 (1999).
17. F. E. Clements and H. Mahfuz, "Proceedings of 16th International Conference on Composite Materials", pp.787-797, 2007.
18. M. Kamibayashi, H. Ogura, and Y. Otsubo, *J. Colloid Interf. Sci*., **321**, 294 (2008).
19. Y. Otsubo, *J. Colloid Interf. Sci.,* **215**, 99 (1999).
20. P. Auroy, L. Auvray, and L. Linger, *J. Colloid Interf. Sci*., **150**, 187 (1992).
21. D. H. Napper, *J. Colloid Interf. Sci*., **58**, 390 (1977).
22. V. S. Stenkamp and J. C. Berg, *Langmuir*, **13**, 3827 (1997).
23. E. B. Zhulina, O. V. Borisov, and V. A. Primitsyn, *J. Colloid Interf. Sci*., **137**, 495 (1990).
24. Y. H. Lin, R. J. Ming, Z. Z. Cheng, Z. J. Peng, W. Q. Mei, and X. Y. Yan, *J. Cent. South Univ. Tech*., **16**, 926 (2009).
25. M. Alizadeh, M.Sc. Dissertation, Islamic Azad University of South Tehran Branch, Tehran, Iran, 2011.
26. D. P. Kalman, R. L. Merrill, N. J. Wagner, and E. D. Wetzel, *Appl. Mat. Int*., **1**, 2602 (2009).
27. T. J. Kang, K. H. Hong, and M. R. Yoo, *Fiber. Polym.*, **11**, 719 (2010).
28. R. G. Egres, M. J. Decker, C. J. Halbach, Y. S. Lee, J. E. Kirkwood, K. M. Kirkwood, and N. J. Wagner, "Proceedings of Army Science Conference", pp.550-555, 2004.
29. H. Rao, M. V. Hosur, J. Mayo, S. Burton, and S. Jeelani, "Proceedings of the SEM Annual Conference", pp.683-693, 2009.